Int. J. Thermal-Fluid Engineering and Modern Energetics 1 (2022) 48-73 www.tfeme-ba.com
doi: 10.51558/2831-0527.2022.1.1.48

Article

Importance of nanofluid evaluations at identical velocity and pumping power: a specific evaluation for Ag-MgO/water hybrid nanofluid flow through a pipe under turbulent regime

Huseyin Kaya [1], Volkan Akgul [1], Cuneyt Uysal [2]
[1]*Mechanical Engineering Department, Faculty of Engineering, Architecture and Design, Bartin University, Bartin, Turkey.*
[2]*Automotive Technologies Program, TOBB Vocational School of Technical Sciences, Karabuk University, Karabuk, Turkey.*

Corresponding author's institutional e-mail address (cuneytuysal@karabuk.edu.tr)

A R T I C L E I N F O

Article history:

Available online 1 July 2022

Keywords:

Entropy generation
Heat convection
Heat transfer enhancement
Nanofluid
Turbulence

A B S T R A C T

In this study, heat transfer and fluid flow characteristics of Ag-MgO/water hybrid nanofluid flow through a pipe were numerically investigated under turbulent regime at identical Reynolds number, velocity and pumping power. To model the flow, the standard $k-\varepsilon$ turbulence model was used. In the analyses, Reynolds number was in the range from Re=10000 to Re=100000 and velocity ranged from V=0.3 m/s to V=3.0 m/s. As a result, it was found that the enhancements in convective heat transfer coefficient were obtained to be 23.72% for identical Reynolds number, 6.27% for identical velocity and 0.44% for identical pumping power. Nanofluids had higher velocities compared to their base fluid to be able to compare them at identical Reynolds number. It was found that this velocity differences can already cause a convective heat transfer enhancement of 16.29% without nanoparticle addition. Nanofluids have higher performance evaluation criteria than unity at identical Reynolds number while they have lower values than unity at identical velocity and pumping power. It can be concluded that the results obtained for identical Reynolds number are extremely optimistic and not realistic. Nanofluids should be examined at identical velocity or pumping power for a fair comparison.

1. Introduction

Studies on nanofluids, which have left their mark on the last decade, still continue to be up-to-date. The most important features of nanofluids, which improve thermal performance in different applications, are the thermophysical properties of the nanoparticles in their structure. Nanofluids, the name given to the homogeneous structures of the base fluid and nanoparticles, are produced using nano-sized particles of metal and non-metal materials. With the addition of nanoparticles, especially the increase in the thermal conductivity value in the base fluid significantly increases the convective heat transfer under flow conditions [1–3]. Convection heat transfer characteristics and thermo-hydraulic performances of nanofluids in in-channel flows or different flow applications (heating-cooling) continue to be intensively investigated experimentally and numerically under laminar and turbulent flow conditions [4–8]. In the 3-D numerical study by Davarnejad et al. [9], the heat transfer performance of MgO/water nanofluid in circular channel was investigated under turbulent flow conditions. Reynolds number range of 3000-19000 and nanoparticle volume fractions of 0.0625%, 0.125%, 0.25%, 0.5% and 1% were used, and the k- model was applied under single-phase, volume of fluid and mixture flow conditions. The highest Nusselt number was obtained with Re 19000 at a 1% volumetric ratio, approximately 35% higher than

pure water under the same conditions. Akbarzadeh et al. [10] performed 2-D pumping power and thermal performance analysis for nanofluid flow in laminar flow conditions in the wavy channel. It was noted that the aspect ratio change increased the Nusselt number and pumping power by approximately 56% and 390%, respectively. Considering the channel aspect ratio, Reynolds number and particle volumetric ratio, it was determined that the dominant parameter on the dimensionless pressure drop parameter was the aspect ratio. The use of nanofluids with low wave amplitude in wavy channels provided the highest heat transfer performance. A numerical study was conducted to examine the variation in heat transfer, pressure drop and entropy generation when graphene-silver/water nanofluid was used as the working fluid instead of pure water in two newly designed microchannel heat sinks. According to the results obtained, it was stated that the nanofluid provides lower surface temperature and thermal resistance than pure water at constant pumping power and higher volume fractions provided more uniform cooling. Bahiraei and Heshmatian [11] pointed out the dominant component in entropy production is the part realized by heat transfer, and lower irreversibility values were obtained with the results of the analysis made with nanofluid. Minea [12] investigated numerically the usage of some water-based hybrid nanofluids as working fluids in a circular channel by considering both laminar and turbulent flow conditions. In the use of nanofluids, the need for high pumping power occurs due to the increased viscosity with the increase in the particle volumetric ratios while the heat transfer increases. These two parameters were examined together, and it was stated that the comparison approach with fixed Re number values was unrealistic. While the highest convection heat transfer coefficient increase was calculated as 20.36% with the hybrid nanofluid combined with 0.5% Al_2O_3 and 1.5% SiO_2, the pumping power increase was obtained as 12% under the same conditions. In addition to aforementioned studies, a more comprehensive literature investigation for generally turbulent flow is given in Table 1.When we look at the studies carried out before, in the analyzes made with nanofluids, higher heat transfer performances were obtained in the same conditions (generally at constant Re number) compared to the case of using base fluids. Comparison studies are usually carried out at a constant Re number. In fact, for nanofluids obtained by adding nanoparticles to a base fluid, thermophysical properties change according to particle type, particle diameter and morphology. In this case, since the thermophysical properties of nanofluids are different at the same Re number, their velocity values are also different (faster), which naturally provides higher convective heat transfer performance [38]. With considering these situations, Uysal [38] analyzed diamond-iron oxide/water hybrid nanofluid flow through rectangular minichannel under laminar flow conditions for identical velocity, mass flow rate, Reynolds number and pumping power. It may be given as a result that hybrid nanofluid showed 30.31% heat transfer improvement when the comparison is realized at identical Reynolds number. However, heat transfer improvement of 2.17% was observed for identical velocity. This situation shows that the studies performed on the identical Reynolds number in the literature present overabundant heat transfer improvement.

In this study, fluid flow and heat transfer characteristics of Ag-MgO/water hybrid nanofluid flow through a pipe were numerically investigated under turbulent regime at identical Reynolds number, velocity, and pumping power. Unlike the study published by Uysal [38], the flow regime, channel geometry and nanofluid type were changed to determine whether the same situation would be observed under these conditions. The results obtained for convective heat transfer coefficient, Nusselt number, Darcy friction factor, entropy generation, Bejan number were presented at identical Reynolds number, velocity, and pumping power and were discussed.

Table 1. Literature survey

Author	Study type	Geometry	Nanofluid	Criteria	Findings
Mohammed et al. [13]	Numerical	Triangular	Ag/water Al_2O_3/water CuO/water diamond/water SiO_2/water TiO_2/water	$\dot{W}$	It was stated that diamond/H_2O nanofluid at 2% by volume had the highest heat transfer coefficient, while Al_2O_3/water had the lowest heat transfer. At identical pumping power (0.005 W), the highest heat transfer coefficient improvement rate of approximately 2% was obtained for SiO_2, CuO, and TiO_2 nanofluids.
Hussein et al. [14]	Numerical Experimental	Circular Elliptic Flat	TiO_2/water	Re	Nusselt number and friction factor were investigated and with the increase of Re number, heat transfer coefficient increased in both base fluid and nanofluid, while friction coefficient decreased. The highest heat transfer coefficient at a volume fraction of 2.5% was obtained as 390 W/m^2K in the flat tube and it was calculated about twice as much as pure water under the same Re number (20000).
Meddah et al. [15]	Experimental	Circular	Al_2O_3/water	Re	Al_2O_3/water nanofluid at a volume fraction of 0.2%-0.9% was used as the working fluid in the double-pipe heat exchanger, and an increase of 1.03 and 4 times, and 1.4 and 2.8 times respectively in heat transfer rate and friction factor, depending on the geometrical change (two different) at 21000 Re number.
Hejazian et al. [16]	Numerical	Circular	TiO_2/water	Re	Three different two-phase models and single-phase model were used, and it was stated that the most reliable results were obtained with the VOF model at low and high-volume fractions for turbulent flow.
Sheikhzadeh et al. [17]	Numerical	Circular	Ag/water Cu/water CuO/water TiO_2/water	Re	The highest entropy generation decrease rate was calculated with 4.0% volume fraction Ag/water nanofluid as 27.28% at Re number 80000 for microchannel.
Siavashi et al. [18]	Numerical	Circular	TiO_2/water	Re	Effect of radius ratio of the channel and volume fraction of nanofluid were investigated and the maximum heat transfer improvement was achieved with 4.0% volume fraction at Re 25000. Also, at Re 10000, maximum Nu number was calculated 40% higher than pure water at radius ratio 0.2.
Huang et al. [19]	Experimental	Corrugated plate	Al_2O_3/water MWCNT/water Al_2O_3-MWCNT/water	V $\dot{W}$	At the same flow rate and pumping power, the heat transfer capacity for the hybrid Al_2O_3-MWCNT/water nanofluid was relatively higher than that of the alumina/water nanofluid. The pressure drop was calculated lower for the hybrid nanofluid than for alumina/water and little higher for pure water.
Uysal et al. [20]	Numerical	Rectangular	ZnO/EG	Re	The highest improvement rate in convective heat transfer with ZnO/EG nanofluid with 4.0% volume fraction was obtained at Re number 10 as 19.33%, and it was stated that the square section was optimum when the channel aspect ratio was taken into account.
Behabadi et al. [21]	Experimental	Circular coil	MWCNT–water	Re	The highest performance evaluation criteria value was calculated as 1.19 with 0.2% weight fraction nanofluid at given Re number.

Table 1. Literature survey (continue)

Author	Study type	Geometry	Nanofluid	Criteria	Findings
Najafabadi et al. [22]	Numerical	Converging circular	Al_2O_3/water	Re	It was seen that Al2O3/water nanofluid has a higher friction factor than water, but when the local entropy generation is considered, it has an improvement effect on the overall system performance. The highest Nu number was obtained approximately 28% higher in the Re number given at a slip length of 10 μm.
Hussein et al. [23]	Numerical	Flat tube	TiO_2/water	Re	While the highest Nu number increase rate was obtained with 4.0% volume fraction nanofluid, approximately 18%, the increase in friction factor was calculated as 12% under the same conditions (Re=100000).
Sheikholeslami et al. [24]	Numerical	Circular	CuO/water	Re $\dot{W}$	Turbulence intensity and Nu number increased with increasing Re number and width ratio. It is stated that better nanofluid mixture can be obtained for lower values of turbulator pitch ratio.
Sheikholeslami et al. [25]	Numerical	Circular	CuO/water	Re	Second law analysis were carried out for single phase nanofluid flow by using turbulators. Effect of revolution angle and Re number were analyzed. Increase in revolution angle provides an enhancement in exergy performance.
Bahmani et al. [26]	Numerical	Circular	Al_2O_3/water	Re	The average Nu number increased by about 32.7% with the use of nanofluid, and the thermal efficiency of the heat exchanger improved by 30% at same Re number. It was stated that the heat exchanger efficiency increase remained constant for higher values of Re number.
Kristiawan et al. [27]	Numerical	Circular	TiO_2/water	Re	When 1.18 vol% TiO_2/water nanofluid was used as the working fluid, the increase in convection heat transfer for Re 1200 was 20.2%, while this value was calculated as 21.87% for Re 14000.
Shahidi et al. [28]	Experimental Numerical	Coil inserted tube	MWCNT-water	Re	With the use of nanofluids, a remarkable improvement of 102% in Nu number was obtained. It was reported that the PEC value was obtained around 1.15 with 0.2% weight fraction nanofluid and minimum hydraulic diameter at Re=20000.
Verma et al. [29]	Experimental	Flat plate collector	CuO/water MgO/water MWCNT/water CuO-MWCNT/ water MgO–MWCNT/ water	$\dot{m}$	Considering the heat transfer and hydraulic performance, optimum working conditions were obtained with 0.75-1.0% volume fraction MgO-MWCNT/water nanofluid. According to the optimum results obtained at 0.025-0.03 kg/s mass flow rate, it was stated that the energy and exergy efficiency of this nanofluid and the collector were calculated as 71.54% and 70.55%, respectively.

Table 1. Literature survey (continue)

Author	Study type	Geometry	Nanofluid	Criteria	Findings
Kaya et al. [30]	Experimental	Evacuated tube collector	ZnO/EG-water	$\dot{m}$	The highest collector efficiency was obtained with 3.0 vol% ZnO/EG-W nanofluid, with the indicated mass flow rate approximately 27% higher than that of pure water. It has been emphasized that there may be stability problems at 4.0 vol% for this nanofluid.
Kaska et al. [31]	Numerical	Flat tube	AIN-Al_2O_3/water	Re	The highest increase in heat transfer coefficient was obtained with 50% for 3.0 vol% nanofluid. The enhancement obtained with 4.0% nanofluid remained lower, which played an important role in determining the optimum value for these operating conditions.
Bazdar et al. [32]	Numerical	Wavy channels	CuO/water	Re	The study was carried out under laminar flow conditions for nanofluid flow in three different wavy channels with different wavelengths. Maximum Nu number enhancement was obtained as 71% with 3.0% volume fraction at Re=7500.
Kanti et al. [33]	Experimental Numerical	Circular	Fly ash/water Fly ash-Cu/water	Re $\dot{W}$	The highest heat transfer coefficient was obtained with hybrid nanofluid, 106% higher than pure water and 17.6% higher than fly ash nanofluid at 2.0 vol%. Additionally, considering the performance evaluation criteria, the value was reached to 1.52 with the hybrid nanofluid.
Shengnan et al. [34]	Numerical	Circular	TiO_2/water	Re	Multi-phase flow of nanofluids at 0.5, 1.0 and 1.5 volume fraction were numerically investigated, and 5 different models were used. The Eulerian-Eulerian model and the Euler-Lagrange model gave more consistent results with the experimental data. A physical explanation of how nanofluids improve heat transfer has been made, and it has been emphasized that the most important phenomenon is the energy and momentum exchange between the phases and the wall.
Shiravi et al. [35]	Experimental	Circular	Carbon nanofluid	Re $\dot{W}$	An enhancement of approximately 40.7% was obtained with a mass fraction of 0.21% in the convection heat transfer coefficient at constant Re number. The friction factor increased as the nanofluid concentration increased and the Re number decreased.

Table 1. Literature survey (continue)

Author	Study type	Geometry	Nanofluid	Criteria	Findings
Mozafarie et al. [36]	Numerical	Circular	Al_2O_3/water	Re	Effect of nanofluids (1.0 vol% and 2.0 vol%) and using fins (different height and pitch) on heat transfer in a double-pipe heat exchanger were investigated. As a result of numerical analyzes performed in Newtonian and Non-Newtonian conditions, 36% and 30% increases in heat transfer were obtained, respectively at given Re number.
Mahani et al. [37]	Numerical	Circular	Cu-Al_2O_3/water	Re	The effect of using the turbulator on nanofluid heat transfer was numerically investigated adopting the multi-phase model. The highest heat transfer capacity improvement was obtained as 97.5% when a twisted rectangular turbulator was used with 4.0 vol% hybrid nanofluid at Re=25000.

2. Material and method

In this study, fluid flow and heat transfer characteristics of Ag-MgO/water hybrid nanofluid flow through a pipe were numerically investigated. The nanoparticle volume fractions were ranged from 0.5% to 2.0% with intervals of 0.5%. The flow was evaluated under turbulent regime. The analyses were performed on identical Reynolds number, velocity, and pumping power. The results obtained by analyses were used to calculate the fluid flow and heat transfer characteristics of nanofluid flow.

2.1. Geometry of channel

Circular cross-sections are the most commonly used geometries in engineering applications. For this reason, researchers and/or engineers are focused on pipes for heat transfer and fluid flow applications. In this study, for nanofluid flow, a pipe having the diameter (D) of 30 mm and length (L) of 1 m was selected. Figure 1 shows the schematic diagram of pipe used in the analyses.

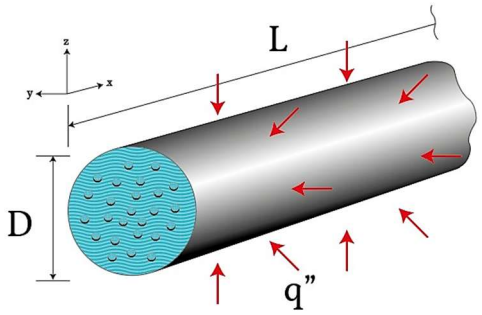

Figure 1. Schematic diagram of hybrid nanofluid flow through a pipe

2.2. Governing equations

The investigation was performed for the range of Re = 10000 and Re = 100000 and for the range of V = 0.3 m/s and V = 3 m/s. These values correspond to turbulent flow. Hence, the flow was considered as turbulent flow and the standard $k-\varepsilon$ turbulence model was used to model the flow.

Turbulence kinetic energy (k) is obtained with solving the following transport equation [39]:

$$\frac{\partial}{\partial t}(\rho k)+\frac{\partial}{\partial x_i}(\rho k u_i)=\frac{\partial}{\partial x_j}\left[\left(\mu+\frac{\mu_t}{\sigma_k}\right)\frac{\partial k}{\partial x_j}\right]+G_k+G_b-\rho\varepsilon-Y_M+S_K \tag{1}$$

where the G_k and G_b terms are the generation of turbulence kinetic energy due to mean velocity gradients and buoyancy, respectively.

Equation 2 gives the transport equation for the dissipation rate of turbulence kinetic energy (ε) [39]:

$$\frac{\partial}{\partial t}(\rho\varepsilon)+\frac{\partial}{\partial x_i}(\rho\varepsilon u_i)=\frac{\partial}{\partial x_j}\left[\left(\mu+\frac{\mu_t}{\sigma_\varepsilon}\right)\frac{\partial\varepsilon}{\partial x_j}\right]+C_{1\varepsilon}\frac{\varepsilon}{k}(G_k+C_{3\varepsilon}G_b)-C_{2\varepsilon}\rho\frac{\varepsilon^2}{k}+S_\varepsilon \tag{2}$$

where the μ_t term is the turbulent viscosity and is expressed as follows:

$$\mu_t=\rho C_\mu\frac{k^2}{\varepsilon} \tag{3}$$

where the C_μ term is a constant and its value was selected to be 0.09 [39]. Similarly, in Equations 1 and 2, the $C_{1\varepsilon}$, $C_{2\varepsilon}$, σ_k, and σ_ε terms are model constants and their values are assumed to be 1.44, 1.92, 1.0, and 1.3, respectively [39].

2.3. Thermophysical properties

In this study, Ag-MgO/water hybrid nanofluid was used as working fluids. In addition, pure water was used as refence fluid for performance comparison. Table 2 shows the thermophysical properties of pure water and Ag and MgO nanoparticles.

Table 2. Thermophysical properties of nanoparticles and pure water [40-41]

Material	ρ (kg/m^3)	C_P (J/kgK)	k (W/mK)	μ (Pas)
Pure Water	995.81	4178.40	0.6172	0.000803
MgO	3560	955	45	-
Ag	10500	235	429	-

For hybrid nanoparticle, it was assumed that the hybrid nanoparticle consists of 50:50 Ag and MgO nanoparticles volumetrically. The density (ρ) and specific heat (C_P) of Ag-MgO hybrid nanoparticle can be determined with the following equations, respectively:

$$\rho_{Ag-MgO}=\frac{\left(\rho_{Ag}W_{Ag}\right)+\left(\rho_{MgO}W_{MgO}\right)}{\left(W_{Ag}+W_{MgO}\right)} \tag{4}$$

$$C_{P,Ag-MgO}=\frac{\left(C_{P,Ag}W_{Ag}\right)+\left(C_{P,MgO}W_{MgO}\right)}{\left(W_{Ag}+W_{MgO}\right)} \tag{5}$$

where the W term denotes the weight of nanoparticles and can be determined with the expression $W=\rho\forall g$. In this expression, the $\forall$ is volume and the g term is gravitation.

The density and specific heat of Ag-MgO/water hybrid nanofluid can be determined with the following equations, respectively:

$$\rho_{hnf} = \varphi\rho_{hnp} + (1-\varphi)\rho_{bf} \tag{6}$$

$$C_{P,hnf} = \varphi C_{P,hnp} + (1-\varphi)C_{P,bf} \tag{7}$$

where the *hnf*, *hnp*, and *bf* subscripts denote hybrid nanofluid, hybrid nanoparticle, and base fluid, respectively.

The thermal conductivity coefficient and dynamic viscosity of Ag-MgO/water hybrid nanofluid can be found with the following correlations, respectively [42]:

$$k_{hnf} = \left(\frac{0.1747\times10^5 + \varphi}{0.1747\times10^5 - 0.1498\times10^6\varphi + 0.1117\times10^7\varphi^2 + 0.1997\times10^8\varphi^3} \right) k_{bf} \tag{8}$$

$$\mu_{hnf} = \left(1 + 32.795\varphi - 7214\varphi^2 + 714600\varphi^3 - 0.1941\times10^8\varphi^4\right)\mu_{bf} \tag{9}$$

These correlations are valid for the nanoparticle volume fraction range of $0 \le \varphi \le 0.02$.

The thermophysical properties of Ag-MgO/water hybrid nanofluid for various nanoparticle volume fractions were tabulated in Table 3.

Table 3. Thermophysical properties of Ag-MgO/water hybrid nanofluid

φ (%)	ρ (kg/m^3)	C_P (J/kgK)	k (W/mK)	μ (Pas)
0.00	995.81	4178.40	0.6172	0.000803
0.50	1034.54	4159.59	0.6437	0.000852
1.00	1073.28	4140.79	0.6696	0.000905
1.50	1112.01	4121.98	0.6938	0.001042
2.00	1150.75	4103.18	0.7150	0.001109

2.4. Numerical procedure

Numerical analyzes were carried out under turbulent flow conditions, and the thermophysical properties of water were used for a temperature of 30 °C. In single-phase turbulent flow conditions, analyzes were performed based on the finite volume method and the near-wall enhancement of the $k-\varepsilon$ turbulence model was used for numerical procedure. In turbulent flow conditions, residual convergence criterion of 10^{-6} and second-order upwind convergence criterion were used for high numerical accuracy. Green – Gauss cell-based method was applied for discretization. 3-D single-phase, incompressible, steady-state fully developed turbulent flow conditions were taken into account for nanofluid flow. The thermophysical properties of the nanofluid were taken as temperature-independent. The inlet temperature of all fluids considered in this study was assumed to be 30°C. In comparison to identical velocity, the inlet velocities were ranged from 0.3 m/s to 3 m/s. Similarly, in comparison to identical Reynolds number, the inlet velocities were determined according the Re= 10000 and Re= 100000 value range of the Reynolds number. As a constant heat flux boundary condition, the $q"$ = 10 kW/m^2 was applied to the outer wall of the pipe, and it was aimed that the thermophysical properties would not change without changing the temperature much.

2.5. Mesh adaptation and code validation

In order to provide the grid-independency for the results, the mesh adaptation procedure was performed. Table 4 shows the variation of Nusselt number with mesh number for pure water.

Table 4. Grid independency test

Mesh Number	*Nu* (-)	Δ*Nu* (%)
12500	557.83	-
25000	535.14	-4.07
37500	576.90	7.80
50000	562.93	-2.42
62500	556.43	-1.15
75000	554.65	-0.32
87500	554.05	-0.11
100000	553.80	-0.05
112500	553.73	-0.01

In order to realize the solution, the mesh model having mesh number of 87500 was selected. The deviation in the Nusselt numbers obtained with the mesh models of 87500 and 100000 was – 0.11%.

The accuracy of selected model was tested with Gnielinski correlation [43] given in Equation 10:

$$Nu = \frac{(f/8)(\mathrm{Re}-1000)\mathrm{Pr}}{1+12.7(f/8)^{1/2}\left(\mathrm{Pr}^{2/3}-1\right)} \tag{10}$$

Figure 2 shows the comparison of the results obtained with selected model and Gnielinski correlation.

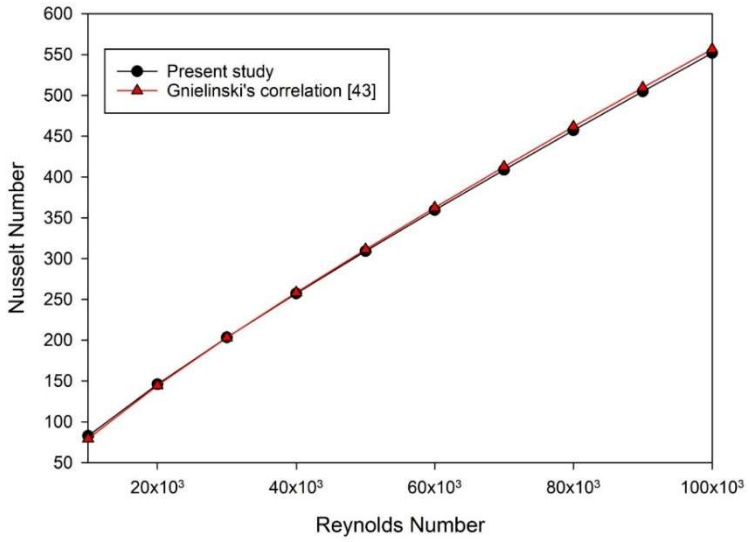

Figure 2. Model accuracy test

According to Figure 2, the highest deviation from Gnielinski correlation was observed to be – 4.26% at Re = 10000. In the remaining Reynolds numbers, the deviations were lower than 1.00%. The average deviation of the model from Gnielinski correlation was determined to be 1.07%.

2.6. Fluid flow and heat transfer characteristics

In this study, fluid flow and heat transfer characteristics of Ag-MgO/water hybrid nanofluid were numerically investigated for identical velocity, Reynolds number, and pumping power.

Reynolds number and pumping power are given as follows, respectively:

$$\mathrm{Re} = \frac{\rho V D_h}{\mu} \tag{11}$$

$$\dot{W} = \dot{\forall}\Delta P \tag{12}$$

In order to determine the heat transfer characteristics of fluid flow, the convective heat transfer coefficient and the Nusselt number can be used. The convective heat transfer coefficient can be calculated as follows:

$$h = \frac{q''}{\left(T_w - T_b\right)} \tag{13}$$

where the T_b term is bulk temperature and can be calculated with the expression $T_b = \left(T_{in} + T_{out}\right)/2$.

Equation 14 presents the Nusselt number:

$$Nu = \frac{hD_h}{k} \tag{14}$$

In order to determine the fluid flow performance of a flow, the Darcy friction factor can be used, and it is expressed with Equation 15:

$$f = 2\frac{D_h}{L}\frac{\Delta P}{\rho V^2} \tag{15}$$

In order to examine the second law performance of a flow, the entropy generation rate can be used. The entropy generation rate for a flow can be divided into two parts: (i) due to heat transfer, and (ii) due to fluid friction. The entropy generation rates per unit length due to heat transfer and due to fluid friction can be expressed as follows:

$$\dot{S}'_{gen,heat\,transfer} = \frac{q''^2\,\pi D_h^2}{kT_b^2 Nu} \tag{16}$$

$$\dot{S}'_{gen,fluid\,friction} = \frac{8\dot{m}^3}{\pi^2\rho^2 T_b}\frac{f}{D_h^5} \tag{17}$$

As can be given in Equation 18, the total entropy generation rate per unit length is obtained with the sum of Equations 16 and 17:

$$\dot{S}'_{gen,total} = \dot{S}'_{gen,heat\,transfer} + \dot{S}'_{gen,fluid\,friction} \tag{18}$$

The Bejan number is a dimensionless number that is effective parameter to evaluate the entropy generation rate. It is defined as the ratio of entropy generation rate due to heat transfer to total entropy generation rate and is expressed as follows:

Performance evaluation criteria (*PEC*) can be defined as follows:

$$PEC = \frac{\left(Nu_{hnf}/Nu_{bf}\right)}{\left(f_{hnf}/f_{bf}\right)^{\frac{1}{3}}} \tag{20}$$

According to the literature, nanoparticle addition to a base fluid enhances convective heat transfer but increases fluid frictions due to increasing viscosity. For this reason, the *PEC* value is important to decide the usage of nanofluids.

3. Results and discussion

In this study, heat transfer and fluid flow characteristics of Ag-MgO/water hybrid nanofluid flow through a pipe were numerically investigated for various nanoparticle volume fractions under turbulence

flow conditions. Convective heat transfer coefficient, the Nusselt number, the Darcy friction factor, entropy generation rate and the Bejan number, performance evaluation criteria values were presented for identical Reynolds number, velocity, and pumping power.

3.1. Fluid flow and heat transfer characteristics

Figures 3a-3c show the variation of convection heat transfer coefficient for different nanoparticle fractions of Ag-MgO/water nanofluid flow with Reynolds number, velocity, and pumping power, respectively.

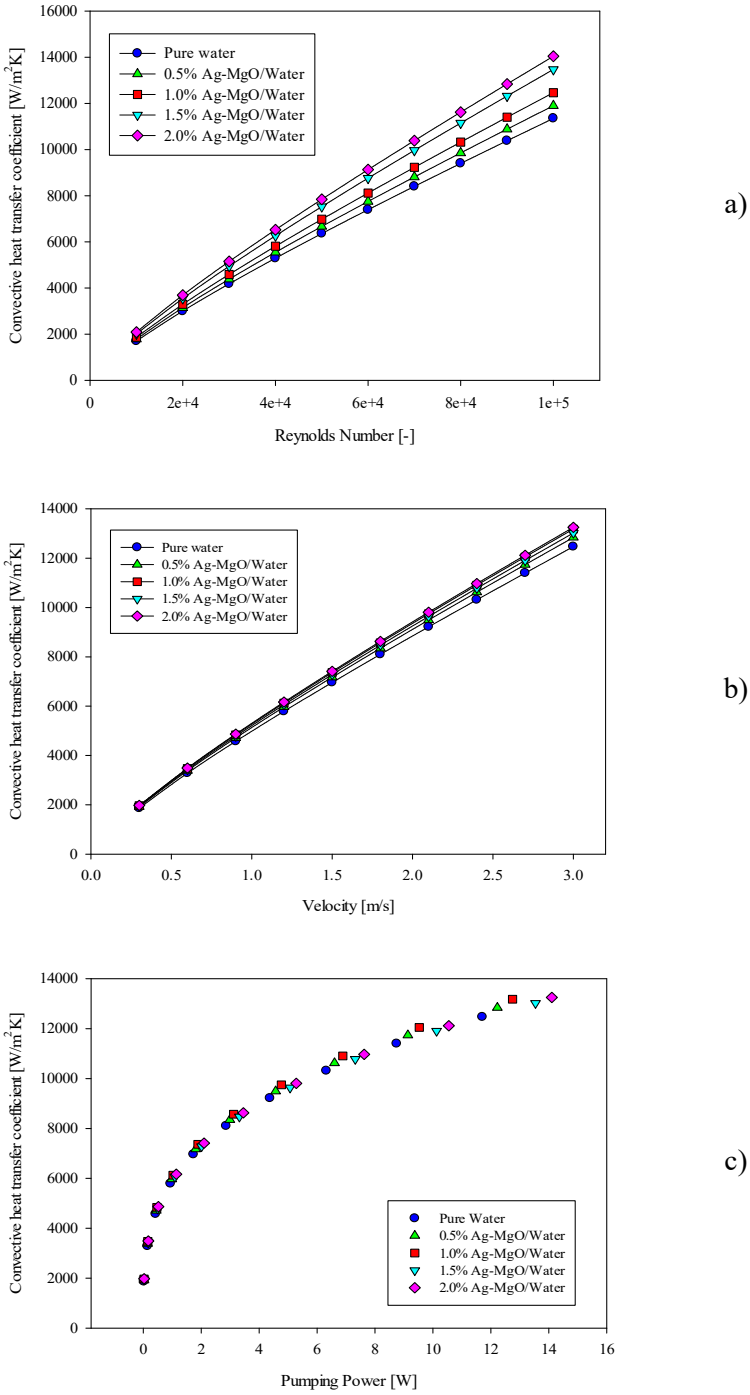

Figure 3. Convective heat transfer coefficient of Ag-MgO/water hybrid nanofluid flow for identical (a) Reynolds number, (b) velocity, and (c) pumping power

According to Figure 3a, at Re = 10000, the convective heat transfer coefficients for pure water and Ag-MgO/water hybrid nanofluid having 2.0% nanoparticle volume fraction were h=1705.12 W/m^{2}K and h=2090.10 W/m^{2}K, respectively. Similarly, these values were obtained to be h=11353.12 W/m^{2}K for pure water and h=14046.03 W/m^{2}K for 2.0% Ag-MgO/water hybrid nanofluid. These mean that 2.0% Ag-MgO hybrid nanoparticle addition to pure water caused to convective heat transfer enhancement of 22.58% and 23.72% at Re = 10000 and Re = 100000, respectively.

In Figure 3b, it was obtained that the convective heat transfer coefficients for pure water at V=0.3 m/s and V=3.0 m/s were h=1864.99 W/m^{2}K and h=12469.68 W/m^{2}K, respectively. These values were found to be h=1976.26 W/m^{2}K and h=13251.18 W/m^{2}K for 2.0% Ag-MgO/water hybrid nanofluid, respectively. These values correspond to 5.97% and 6.27% convective heat transfer enhancement with 2.0% Ag-MgO hybrid nanoparticle addition to pure water at V= 0.3 m/s and V= 3.0 m/s, respectively.

In Figure 3c, the pumping power was selected to be $\dot{W}$ = 10 W for comparison and the values were determined with interpolation. At $\dot{W}$ = 10 W, the convective heat transfer coefficient was determined to be h=11849.92 W/m^{2}K for pure water and h=11902.35 W/m^{2}K for 2.0% Ag-MgO hybrid nanofluid. This corresponds to a convective heat transfer enhancement of 0.44%.

3.2. Nusselt number

Figures 4a-4c show the variation of Nusselt number for different nanoparticle fractions of Ag-MgO/water nanofluid flow with Reynolds number, velocity, and pumping power, respectively.

In Figure 4a, the Nusselt number values were obtained to be Nu = 82.88 for pure water and Nu = 87.70 for 2.0% Ag-MgO hybrid nanofluid at Re = 10000. This corresponds to an increase of 5.97% in the Nusselt number. Similarly, at Re = 100000, the Nusselt number values were found to be Nu = 551.84 for pure water and Nu = 589.34 for 2.0% Ag-MgO hybrid nanofluid. This also correspond to an increase of 6.80% in the Nusselt number. However, according to Figure 4b, the Nusselt number values were Nu = 90.65 for pure water and Nu = 82.92 for 2.0% Ag-MgO hybrid nanofluid at V = 0.3 m/s. This is a decrement of 8.53% for the Nusselt number. Similarly, at V = 3.0 m/s, the Nusselt number values were Nu=606.11 for pure water and Nu = 555.99 for 2.0% Ag-MgO hybrid nanoparticle. This corresponds to a decrement of 8.27% in the Nusselt number. Similar situation was also observed for identical pumping power. At 10 W, the Nusselt number was obtained to be Nu = 575.98 for pure water and Nu = 499.40 for 2.0% Ag-MgO hybrid nanofluid. This corresponds to a decrement of 13.30% in the Nusselt number.

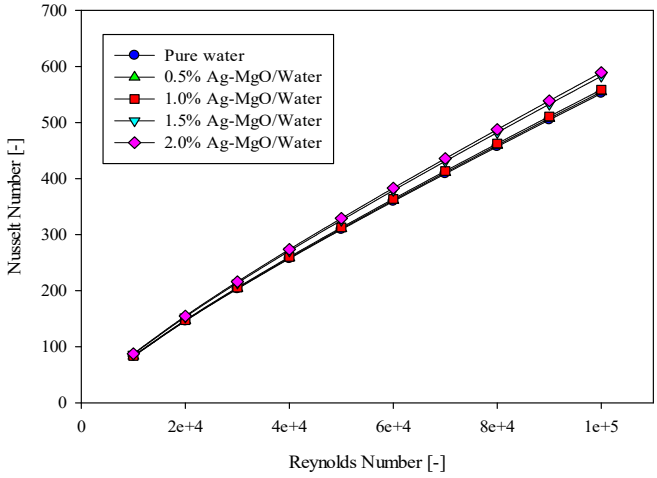

a)

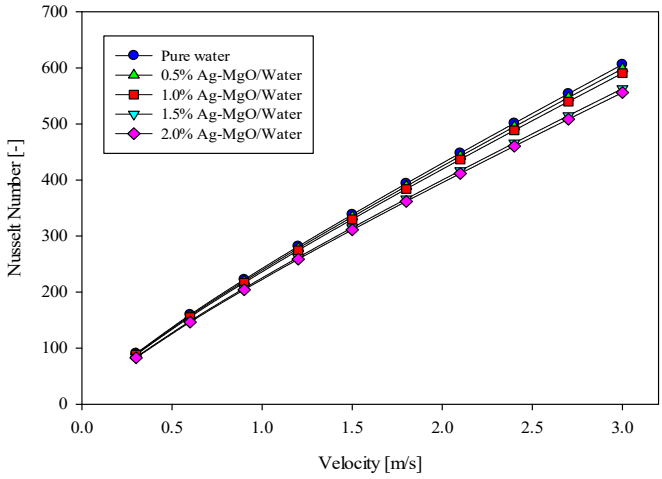

b)

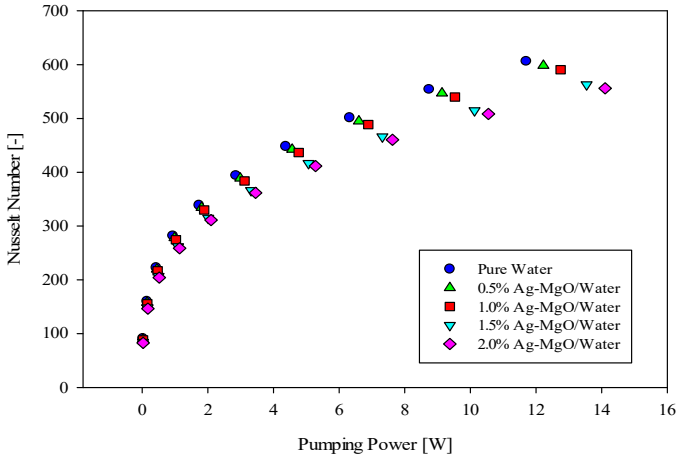

c)

Figure 4. Nusselt number of Ag-MgO/water hybrid nanofluid flow for identical (a) Reynolds number, (b) velocity, and (c) pumping power

3.3. Darcy friction factor

The variation of Darcy friction factor for different nanoparticle fractions of Ag-MgO/water nanofluid flow with Reynolds number, velocity, and pumping power were shown in Figures 5a-5c, respectively.

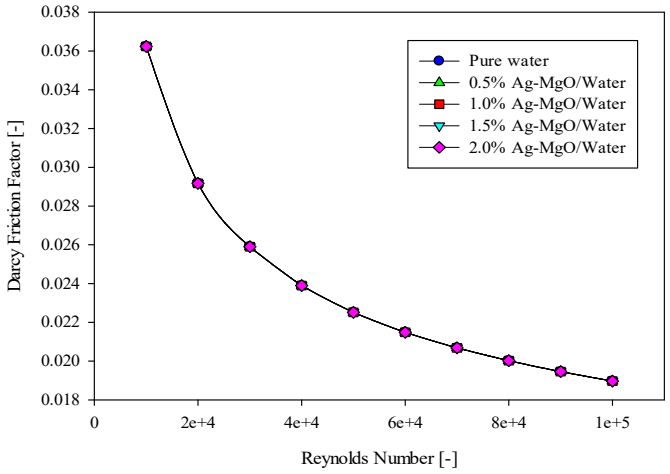

a)

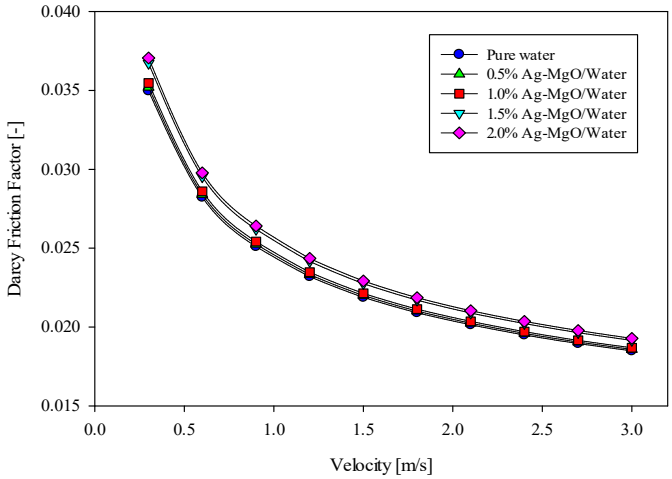

b)

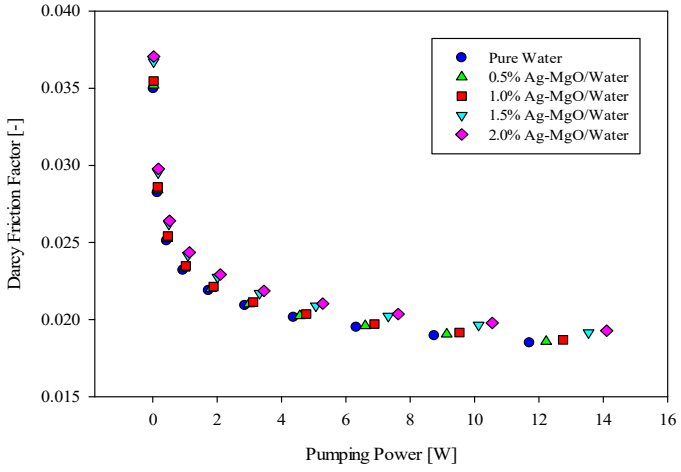

c)

Figure 5. Darcy friction factor of Ag-MgO/water hybrid nanofluid flow for identical (a) Reynolds number, (b) velocity, and (c) pumping power

In Figure 5a, it was obtained that the Darcy friction factor values for all fluids considered in this study were equal. However, in Figure 5b, it was observed that the Darcy friction factor increases with increase in nanoparticle volume fraction. At V=0.3 m/s, the Darcy friction factor was f = 0.034970 for pure water and f = 0.037064 for 2.0% Ag-MgO hybrid nanofluid. Similarly, at V = 3.0 m/s, the Darcy friction factor was found to be f = 0.018491 for pure water and f = 0.019280 for 2.0% Ag-MgO hybrid nanofluid. It can be concluded for identical velocity that the 2.0% Ag-MgO hybrid nanoparticle addition to pure water caused to 5.99% and 4.27% increases in the Darcy friction factor at V=0.3 m/s and V=3.0 m/s, respectively. According to Figure 5c, at $\dot{W}$ =10 W, the Darcy friction factors for pure water and 2.0% Ag-MgO hybrid nanofluid were determined to be f = 0.018759 and f = 0.019892, respectively. This means that 2.0% Ag-MgO hybrid nanoparticle addition to pure water caused to an increase of 6.04% in the Darcy friction factor at pumping power of 10 W.

3.4. Entropy generation rate

Figures 6a-6c show the variation of entropy generation rate per unit length due to heat transfer for different nanoparticle fractions of Ag-MgO/water nanofluid flow with Reynolds number, velocity, and pumping power, respectively.

According to Figure 6a, the entropy generation rates per unit length due to heat transfer decreased with increase in the nanoparticle volume fraction and its values for pure water at Re=10000 and Re=100000 were obtained to be $\dot{S}'_{gen,heat\ transfer}$ = 59.74×10^{-3} W/mK and $\dot{S}'_{gen,heat\ transfer}$ =9.03×10^{-3} W/mK, respectively. These values for 2.0% Ag-MgO/water nanofluid were obtained to be $\dot{S}'_{gen,heat\ transfer}$ = 48.81×10^{-3} W/mK and $\dot{S}'_{gen,heat\ transfer}$ = 7.30×10^{-3} W/mK, respectively. It means that 2.0% Ag-MgO hybrid nanoparticle addition to pure water caused to a decrease of 18.30% at Re = 10000 and a decrease of 19.15% at Re = 100000 in the entropy generation rate per unit length due to heat transfer. As can be seen from Figure 6b, these ratios were not that high. At V = 0.3 m/s and V=3.0 m/s, the entropy generation rates per unit length due to heat transfer for pure water were $\dot{S}'_{gen,heat\ transfer}$ = 54.63×10^{-3} W/mK and $\dot{S}'_{gen,heat\ transfer}$ = 8.22×10^{-3} W/mK, respectively. These values were $\dot{S}'_{gen,heat\ transfer}$ = 51.60×10^{-3} W/mK and $\dot{S}'_{gen,heat\ transfer}$ = 7.74×10^{-3} W/mK, respectively. These values correspond to a decrease of 5.55% at V=0.3 m/s and a decrease of 5.89% at V=3.0 m/s in the entropy generation rate per unit length due to heat transfer. In Figure 6c, it was seen that the entropy generation rates per unit length due to heat transfer for all fluids considered in this study were almost the same at higher pumping powers. At $\dot{W}$ = 10 W, the entropy generation rates per unit length due to heat transfer for pure water and 2.0% Ag-MgO hybrid nanofluid were $\dot{S}'_{gen,heat\ transfer}$ = 8.67 10^{-3} W/mK and $\dot{S}'_{gen,heat\ transfer}$ = 8.63 10^{-3} W/mK, respectively.

Figures 7a-7c show the variation of entropy generation rate per unit length due to fluid friction for different nanoparticle fractions of Ag-MgO/water nanofluid flow with Reynolds number, velocity, and pumping power, respectively.

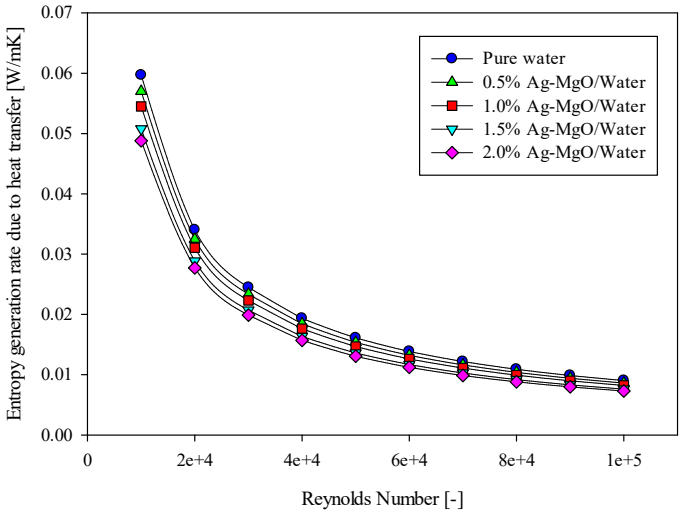

a)

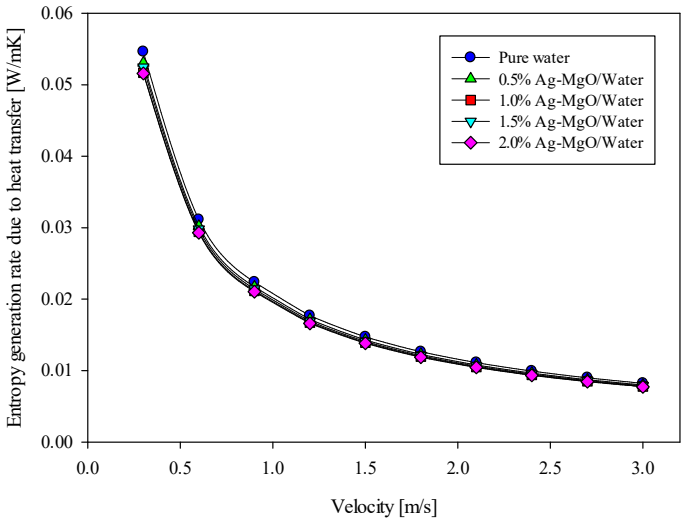

b)

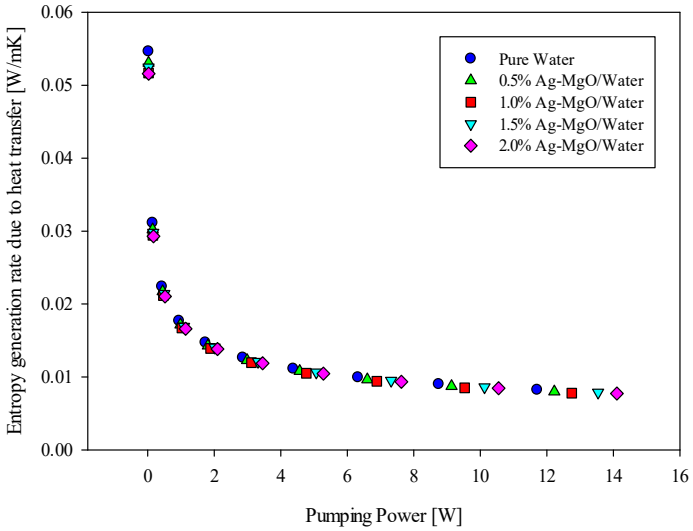

c)

Figure 6. Entropy generation rate per unit length due to heat transfer of Ag-MgO/water hybrid nanofluid flow for identical (a) Reynolds number, (b) velocity, and (c) pumping power

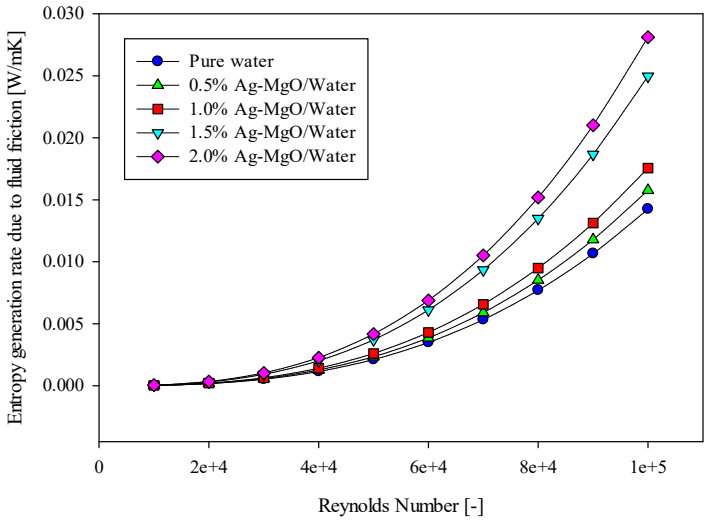

a)

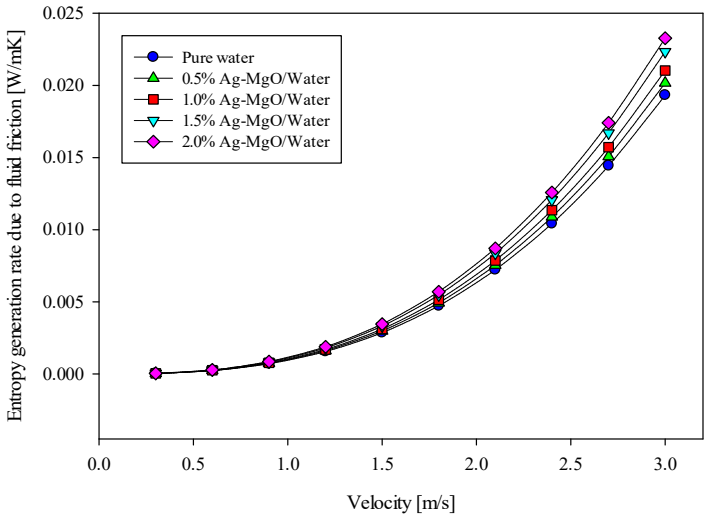

b)

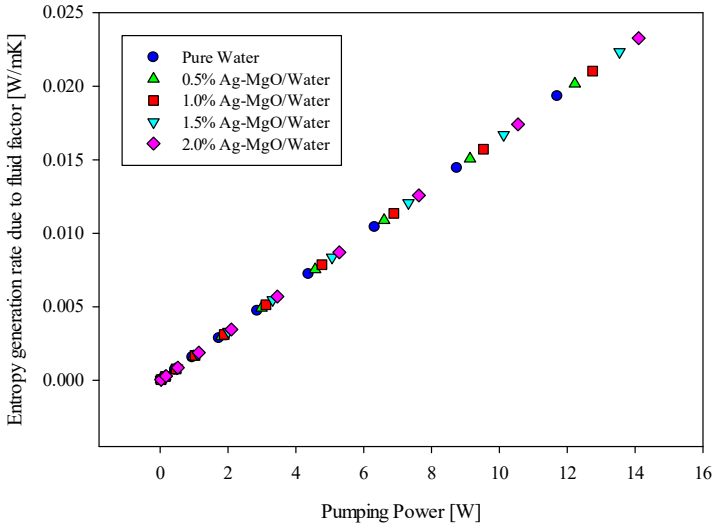

c)

Figure 7. Entropy generation rate per unit length due to fluid friction of Ag-MgO/water hybrid nanofluid flow for identical (a) Reynolds number, (b) velocity, and (c) pumping power

In Figure 7a, the entropy generation rates per unit length due to fluid friction increased with increase in the nanoparticle volume fraction and its values for pure water at Re = 10000 and Re = 100000 were obtained to be $\dot{S}'_{gen,\,fluid\,friction} = 2.71\times10^{-5}$ W/mK and $\dot{S}'_{gen,\,fluid\,friction} = 14.25\times10^{-3}$ W/mK, respectively. Similarly, these values were obtained to be $\dot{S}'_{gen,\,fluid\,friction} = 5.36\times10^{-5}$ W/mK and $\dot{S}'_{gen,\,fluid\,friction} = 28.11\times10^{-3}$ W/mK, respectively. It is said that 2.0% Ag-MgO hybrid nanoparticle addition to pure water caused to 97.79% and 97.26% increase in the entropy generation rates per unit length due to fluid friction at Re = 10000 and Re = 100000, respectively. In Figure 7b, at V = 0.3 m/s, the entropy generation rates per unit length due to fluid friction were $\dot{S}'_{gen,\,fluid\,friction} = 3.67\times10^{-5}$ W/mK for pure water and $\dot{S}'_{gen,\,fluid\,friction} = 4.46\times10^{-5}$ W/mK for 2.0% Ag-MgO/water hybrid nanofluid. This corresponds to an increase of 21.52%. At V=3.0 m/s, pure water and 2.0% Ag-MgO/water hybrid nanofluid had $\dot{S}'_{gen,\,fluid\,friction} = 19.31\times10^{-3}$ W/mK and $\dot{S}'_{gen,\,fluid\,friction} = 23.27\times10^{-3}$ W/mK, respectively. This corresponds to an increase of 20.51%. In Figure 3c, the same values were obtained. As a result, at $\dot{W} = 10$ W, pure water and 2.0% Ag-MgO/water hybrid nanofluid had the same $\dot{S}'_{gen,\,fluid\,friction}$ value of 16.50×10^{-3} W/mK.

The variation of total entropy generation rates per unit length for different nanoparticle fractions of Ag-MgO/water nanofluid flow with Reynolds number, velocity, and pumping power, respectively was shown in Figure 8a-8c.

In Figures 8a-8c, the total entropy generation rates for all fluids decreased until a certain value and then started to increase. In Figure 8a, the minimum total entropy generation rates for pure water and 0.5% Ag-MgO/water hybrid nanofluid were obtained at V=1.8 m/s, whereas they were obtained at V=1.5 m/s for the remaining fluids. In Figure 8b, the minimum total entropy generation rates were observed at Re=60000 for pure water and 0.05% and 1.0% Ag-MgO/water hybrid nanofluid, but these values were observed at Re=50000 for the remaining fluids. Moreover, in Figures 8a and 8b, pure water had the highest total entropy generation rate values until this certain value and the total entropy generation value decreased with increase in the nanoparticle volume fraction. However, after this certain value, pure water had the minimum total entropy generation rate and the total entropy generation rate increased with increase in the nanoparticle volume fraction. As a result, at Re = 10000, pure water had $\dot{S}'_{gen,total} = 59.73\times10^{-3}$ W/mK while 2.0% Ag-MgO/water had $\dot{S}'_{gen,total} = 48.86\times10^{-3}$ W/mK. However, at Re=100000, pure water had $\dot{S}'_{gen,total} = 23.28\times10^{-3}$ W/mK while 2.0% Ag-MgO/water hybrid nanofluid had $\dot{S}'_{gen,total} = 35.41\times10^{-3}$ W/mK. Similar trend of total entropy generation rate was reported for laminar flow conditions by Uysal [38] and Uysal et al. [44].

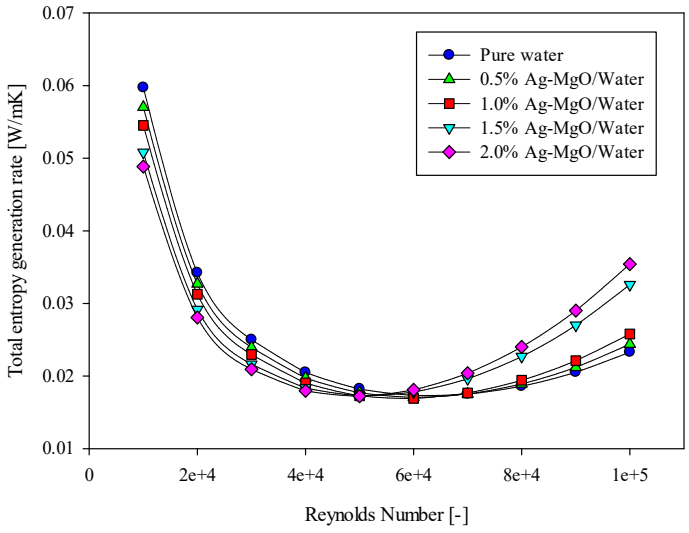

a)

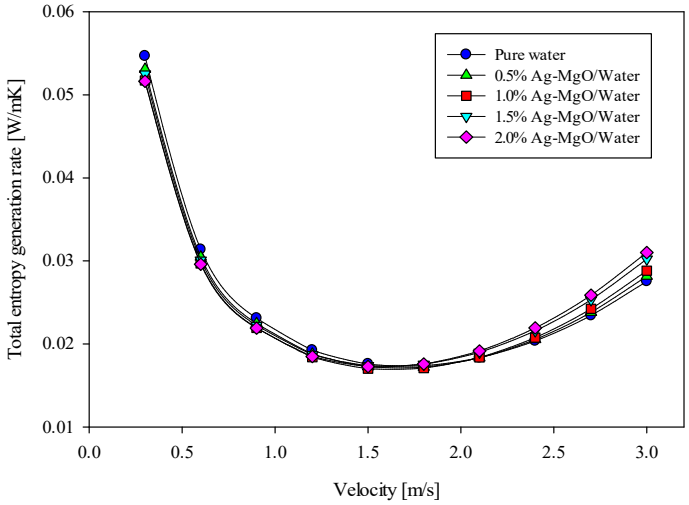

b)

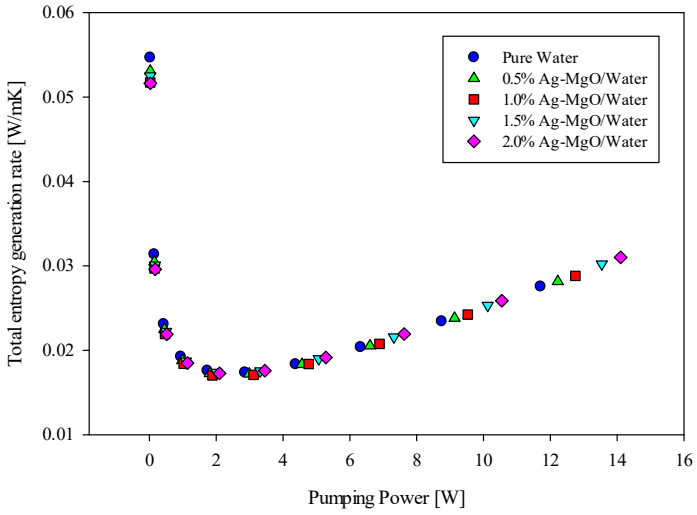

c)

Figure 8. Total entropy generation rate per of Ag-MgO/water hybrid nanofluid flow for identical (a) Reynolds number, (b) velocity, and (c) pumping power

3.5. Bejan number

Figures 9a-9c show the variation of Bejan number for different nanoparticle fractions of Ag-MgO/water nanofluid flow with Reynolds number, velocity, and pumping power, respectively.

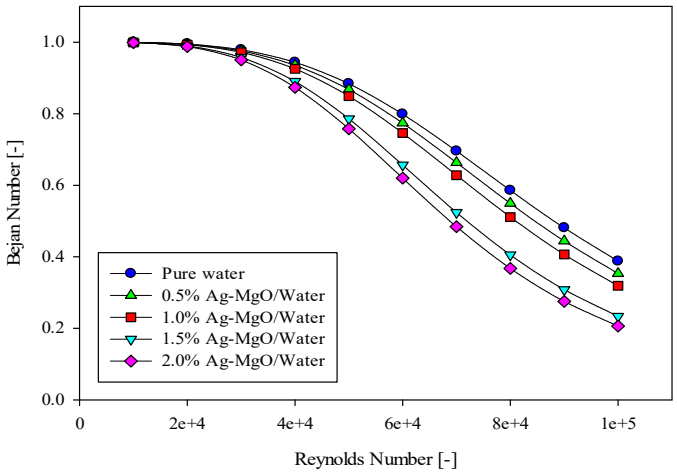

a)

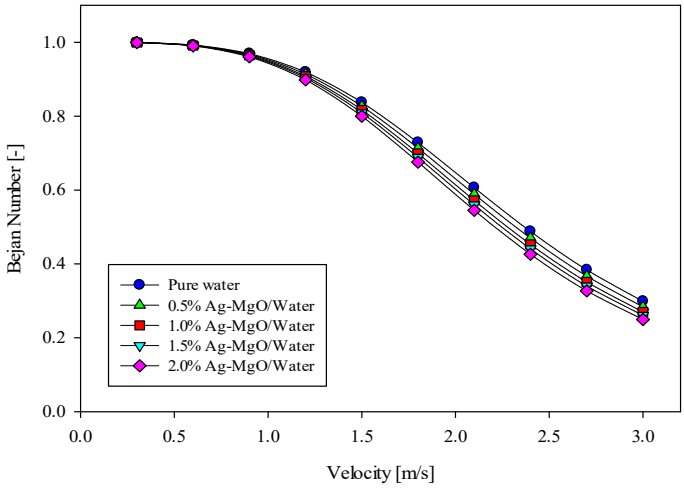

b)

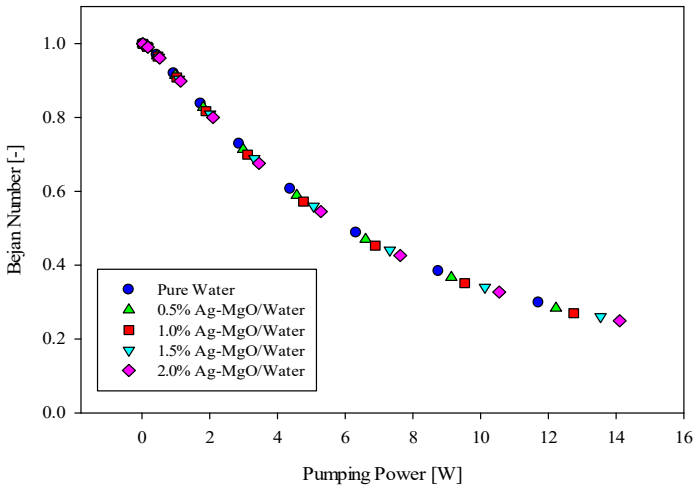

c)

Figure 9. Bejan number of Ag-MgO/water hybrid nanofluid flow for identical (a) Reynolds number, (b) velocity, and (c) pumping power

In Figures 9a-9c, the Bejan number of flows decreased with increase in the nanoparticle volume fraction. This decrease was higher at identical Reynolds number compared to that of identical velocity. However, at identical pumping power, this decrease is even lower. At Re = 100000, the Bejan numbers for pure water and 2.0% Ag-MgO/water hybrid nanofluid were Be = 0.3879 and Be = 0.2062, respectively. It means that 2.0% Ag-MgO hybrid nanoparticle addition to pure water caused to a decrease of 46.84% in the Bejan number. Similarly, at V = 3.0 m/s, pure water had Be = 0.2986 and 2.0% Ag-MgO/water hybrid nanofluid had Be = 0.2495. This corresponds to a decrease of 16.44%. At $\dot{W}$ = 10 W, the Bejan number of pure water was Be = 0.3479 and that of 2.0% Ag-MgO/water hybrid nanofluid was Be = 0.3458. This corresponds to a decrease of only 0.60%.

3.6. Performance evaluation criteria

The variation of performance evaluation criteria for different nanoparticle fractions of Ag-MgO/water nanofluid flow with Reynolds number, velocity, and pumping power, respectively was shown in Figures 10a-10c.

Higher PEC value than unity for a nanofluid means that the nanofluid has higher performance compared to its base fluid. In Figure 10a, all nanofluids had higher PEC values than unity. The PEC values were increased with increase in the nanoparticle volume fraction. At Re = 10000, 2.0% Ag-MgO/water hybrid nanofluid had PEC = 1.07. However, according to Figure 10b, all nanofluids had lower PEC values than unity and the PEC values decreased with increase in the nanoparticle volume fraction. At V=3.0 m/s, 2.0% Ag-MgO/water hybrid nanofluid had PEC = 0.93. Similarly, in Figure 10c, all nanofluids had lower PEC values than unity and the PEC values decreased with increase in the nanoparticle volume fraction. At $\dot{W}$ = 10 W, the PEC value of 2.0% Ag-MgO/water hybrid nanofluid was PEC = 0.91.

According to the results, one can think that nanofluids are better performances compared to their base fluids when nanofluids are compared at identical Reynolds number. However, the results obtained at identical velocities and pumping powers show the opposite.

As can be seen from Equation 11, the Reynolds number is function of density and viscosity. And, nanoparticle addition to base fluid changes its density and viscosity. It means that comparison at identical Reynolds number does not correspond to comparison at identical velocity. Table 5 shows the velocity values corresponding to Reynolds number for all fluids considered in this study.

As can be seen from Table 5, velocity values increase with increase in nanoparticle volume fraction at identical Reynolds numbers. As a result, at Re = 60000, pure water had V = 1.6128 m/s and 2.0% Ag-MgO/water hybrid nanofluid had V = 1.9274 m/s. The velocity value of 1.9274 m/s corresponds to about Re = 71705 for pure water. At Re = 60000 and Re = 70000, the convective heat transfer coefficients for pure water were obtained to be h = 6359.26 W/m^{2}K and h = 7395.03 W/m^{2}K, respectively. Even in pure water, this velocity difference caused to an increase of 16.29% in the convective heat transfer coefficient. It can be concluded that comparison nanofluids at identical Reynolds number is not a fair comparison procedure.

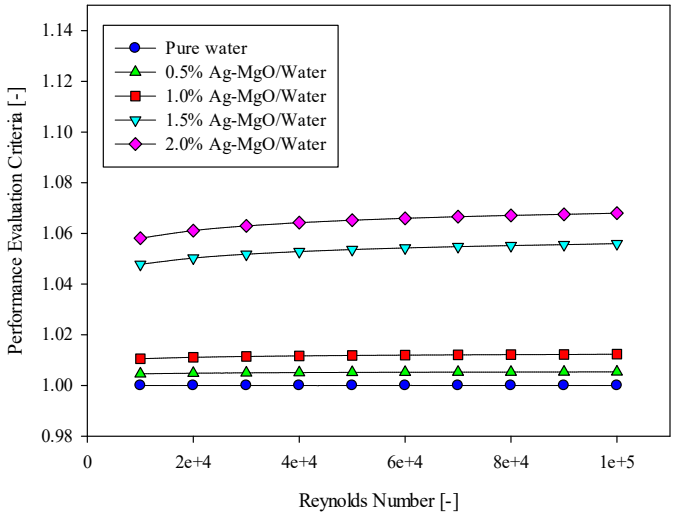

a)

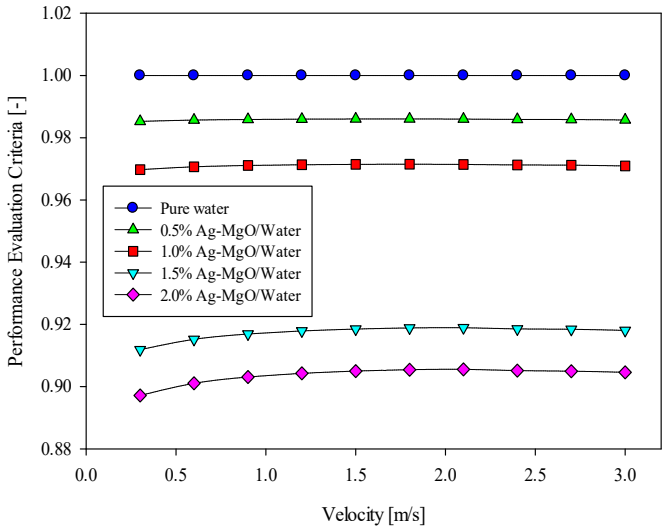

b)

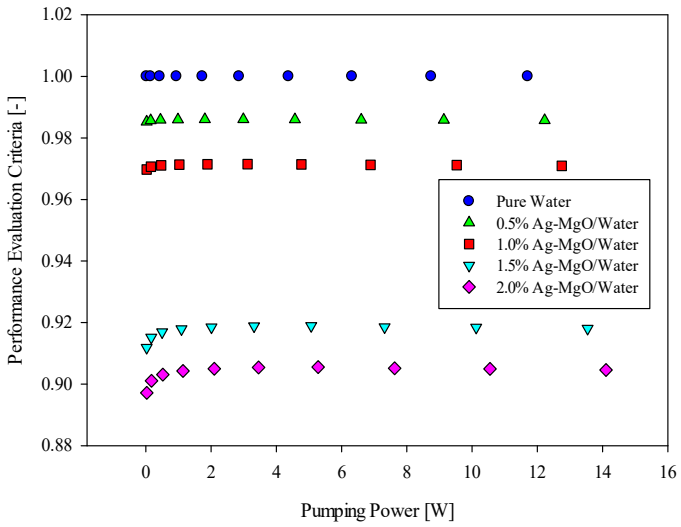

c)

Figure 10. Performance evaluation criteria of Ag-MgO/water hybrid nanofluid flow for identical (a) Reynolds number, (b) velocity, and (c) pumping power

As can be seen from Equation 11, the Reynolds number is function of density and viscosity. And, nanoparticle addition to base fluid changes its density and viscosity. It means that comparison at identical Reynolds number does not correspond to comparison at identical velocity. Table 5 shows the velocity values corresponding to Reynolds number for all fluids considered in this study.

As can be seen from Table 5, velocity values increase with increase in nanoparticle volume fraction at identical Reynolds numbers. As a result, at Re = 60000, pure water had V = 1.6128 m/s and 2.0% Ag-MgO/water hybrid nanofluid had V = 1.9274 m/s. The velocity value of 1.9274 m/s corresponds to about Re = 71705 for pure water. At Re = 60000 and Re = 70000, the convective heat transfer coefficients for pure water were obtained to be h = 6359.26 W/m^{2}K and h = 7395.03 W/m^{2}K, respectively. Even in pure water, this velocity difference caused to an increase of 16.29% in the convective heat transfer coefficient. It can be concluded that comparison nanofluids at identical Reynolds number is not a fair comparison procedure.

Table 5. Velocities corresponding to Reynolds numbers for all fluids considered in this study.

Fluids	Velocity (m/s)									
	Re=10000	Re=20000	Re=30000	Re=40000	Re=50000	Re=60000	Re=70000	Re=80000	Re=90000	Re=100000
Pure water	0.2688	0.5376	0.8064	1.0752	1.3440	1.6128	1.8816	2.1503	2.4191	2.6879
0.5% Ag-MgO/water	0.2745	0.5490	0.8236	1.0981	1.3726	1.6471	1.9216	2.1961	2.4707	2.7452
1.0% Ag-MgO/water	0.2811	0.5621	0.8432	1.1243	1.4053	1.6864	1.9675	2.2486	2.5296	2.8107
1.5% Ag-MgO/water	0.3123	0.6247	0.9370	1.2494	1.5617	1.8741	2.1864	2.4988	2.8111	3.1235
2.0% Ag-MgO/water	0.3212	0.6425	0.9637	1.2850	1.6062	1.9274	2.2487	2.5699	2.8912	3.2124

4. Conclusions

In this study, heat transfer and fluid flow characteristics of Ag-MgO/water hybrid nanofluid flow through a pipe were numerically investigated at identical Reynolds number, velocity and pumping power under turbulent flow conditions. The obtained results show that 2.0% Ag-MgO hybrid nanoparticle addition to pure water caused to 23.72%, 6.27%, and 0.44% convective heat transfer enhancements at identical Reynolds number, velocity, and pumping power. In addition, lower PEC values than unity were obtained for all nanofluids at identical velocity and pumping power. Comparison at identical Reynolds number is not a fair comparison method due to that Reynolds number is function of density and viscosity and higher velocities are obtained for nanofluids. For this reason, the results reported for identical Reynolds number, which constitutes almost all of the literature, present overabundant convective heat transfer enhancements. Nanofluids should be compared at identical velocities or pumping powers for a fair comparison. For future studies, other nanofluid types that are claimed to cause so much convective heat transfer enhancement should be investigated.

References

[1] Bianco V, Chiacchio F, Manca O, Nardini S. “Numerical investigation of nanofluids forced convection in circular tubes”. Applied Thermal Engineering 29, 3632–3642, 2009.

[2] Vajjha RS, Das DK. “Experimental determination of thermal conductivity of three nanofluids and development of new correlations”. International Journal of Heat and Mass Transfer 52, 4675–4682, 2009.

[3] Uysal C, Korkmaz E. “Estimation of entropy generation for Ag-MgO/water hybrid nanofluid flow through rectangular minichannel by using artificial neural network”. Journal of Polytechnic 22 (1), 41-51, 2019.

[4] Al-Baghdadi MARS, Noor ZMH, Zeiny A, Burns A, Wen D. “CFD analysis of a nanofluid-based microchannel heat sink”. Thermal Science and Engineering Progress 20, 100685, 2020.

[5] Alshayji A, Asadi A, Alarifi IM. "On the heat transfer effectiveness and pumping power assessment of a diamond-water nanofluid based on thermophysical properties: An experimental study". Powder Technology 373, 397–410, 2020.

[6] Sheikholeslami M, Farshad SA, Shafee A, Tlili I. "Modeling of solar system with helical swirl flow device considering nanofluid turbulent forced convection". Physica A: Statistical Mechanics and its Applications 550, 123952, 2020.

[7] Bahiraei M, Heshmatian S, Goodarzi M, Moayedi H. "CFD analysis of employing a novel ecofriendly nanofluid in a miniature pin fin heat sink for cooling of electronic components: Effect of different configurations". Advanced Powder Technology 30, 2503–2516, 2019.

[8] Sheikholeslami M, Jafaryar M, Ali JA, Hamad SM, Divsalar A, Shafee A, Nguyen-Thoi T, Li Z. "Simulation of turbulent flow of nanofluid due to existence of new effective turbulator involving entropy generation". Journal of Molecular Liquids 291, 111283, 2019.

[9] Davarnejad R, Jamshidzadeh M. "CFD modeling of heat transfer performance of MgO-water nanofluid under turbulent flow". Engineering Science and Technology, an International Journal 18, 536–542, 2015.

[10] Akbarzadeh M, Rashidi S, Bovand M, Ellahi R. "A sensitivity analysis on thermal and pumping power for the flow of nanofluid inside a wavy channel". Journal of Molecular Liquids 220, 1–13, 2016.

[11] Bahiraei M, Heshmatian S. "Thermal performance and second law characteristics of two new microchannel heat sinks operated with hybrid nanofluid containing graphene-silver nanoparticles". Energy Conversion and Management 168, 357–370, 2018.

[12] Minea AA. "Pumping power and heat transfer efficiency evaluation on Al2O3, TiO2 and SiO2 single and hybrid water-based nanofluids for energy application". Journal of Thermal Analysis and Calorimetry 139, 1171–1181, 2020.

[13] Mohammed HA, Gunnasegaran P, Shuaib NH. "The impact of various nanofluid types on triangular microchannels heat sink cooling performance". International Communications in Heat and Mass Transfer 38, 767–773, 2011.

[14] Hussein AM, Sharma K V., Bakar RA, Kadirgama K. "The effect of cross sectional area of tube on friction factor and heat transfer nanofluid turbulent flow". International Communications in Heat and Mass Transfer 47, 49–55, 2013.

[15] Maddah H, Alizadeh M, Ghasemi N, Wan Alwi SR. "Experimental study of Al2O3/water nanofluid turbulent heat transfer enhancement in the horizontal double pipes fitted with modified twisted tapes". International Journal of Heat Mass Transfer 78, 1042–1054, 2014.

[16] Hejazian M, Moraveji MK, Beheshti A. "Comparative numerical investigation on TiO2/water nanofluid turbulent flow by implementation of single phase and two phase approaches". Numerical Heat Transfer, Part A: Applications 66, 330–348, 2014.

[17] Sheikhzadeh G, Aghaei A, Ehteram H, Abbaszadeh M. "Analytical study of parameters affecting entropy generation of nanofluid turbulent flow in channel and micro-channel". Thermal Science 20, 2037–2050, 2016.

[18] Siavashi M, Jamali M. "Heat transfer and entropy generation analysis of turbulent flow of TiO_2-water nanofluid inside annuli with different radius ratios using two-phase mixture model". Applied Thermal Engineering 100, 1149–1160, 2016.

[19] Huang D, Wu Z, Sunden B. "Effects of hybrid nanofluid mixture in plate heat exchangers". Experimental Thermal and Fluid Science 72, 190–196, 2016.

[20] Uysal C, Arslan K, Kurt H. "A numerical analysis of fluid flow and heat transfer characteristics of ZnO-ethylene glycol nanofluid in rectangular microchannels". Strojniški Vestnik – Journal of Mechanical Engineering 62, 603–613, 2016.

[21] Akhavan-Behabadi MA, Shahidi M, Aligoodarz MR, Ghazvini M. "Experimental investigation on thermo-physical properties and overall performance of MWCNT–water nanofluid flow inside horizontal coiled wire inserted tubes". Heat and Mass Transfer 53, 291–304, 2017.

[22] Najafabadi HH, Moraveji MK. "CFD investigation of local properties of Al2O3/water nanofluid in a converging microchannel under imposed pressure difference". Advanced Powder Technology 28:763–774, 2017.

[23] Hussein AM, Dawood HK, Bakara RA, Kadirgamaa K. "Numerical study on turbulent forced convective heat transfer using nanofluids TiO2 in an automotive cooling system". Case Studies in Thermal Engineering 9, 72–78, 2017.

[24] Sheikholeslami M, Jafaryar M, Shafee A, Li Z. "Investigation of second law and hydrothermal behavior of nanofluid through a tube using passive methods". Journal of Molecular Liquids 269, 407–416, 2018.

[25] Sheikholeslami M, Jafaryar M, Ganji DD, Li Z. "Exergy loss analysis for nanofluid forced convection heat transfer in a pipe with modified turbulators". Journal of Molecular Liquids 262, 104–110, 2018.

[26] Bahmani MH, Sheikhzadeh G, Zarringhalam M, Akbari OA, Alrashed AAAA, Shabani GAS, Goodarzi M. "Investigation of turbulent heat transfer and nanofluid flow in a double pipe heat exchanger". Advanced Powder Technology 29, 273–282, 2018.

[27] Kristiawan B, Santoso B, Wijayanta AT, Aziz M, Miyazaki T. "Heat transfer enhancement of TiO_2/water nanofluid at laminar and turbulent flows: A numerical approach for evaluating the effect of nanoparticle loadings". Energies 11 (6), 11061584, 2018.

[28] Shahidi M, Aligoodarz MR, Akhavan-Behabadi MA, Foroutani S, Rahbari A. "Experimental and numerical investigation on turbulent flow of multiwall carbon nanotube-water nanofluid inside vertical coiled wire inserted tubes". Thermal Science 22, 125–136, 2018.

[29] Verma SK, Tiwari AK, Tiwari S, Chauhan DS. "Performance analysis of hybrid nanofluids in flat plate solar collector as an advanced working fluid". Solar Energy 167, 231–241, 2018.

[30] Kaya H, Arslan K, Eltugral N. "Experimental investigation of thermal performance of an evacuated U-Tube solar collector with ZnO/Ethylene glycol-pure water nanofluids". Renewable Energy 122, 329–338, 2018.

[31] Kaska SA, Khalefa RA, Hussein AM. "Hybrid nanofluid to enhance heat transfer under turbulent flow in a flat tube". Case Studuies in Thermal Engineering 13, 4–13, 2019.

[32] Bazdar H, Toghraie D, Pourfattah F, Akbari OA, Nguyen HM, Asadi A. "Numerical investigation of turbulent flow and heat transfer of nanofluid inside a wavy microchannel with different wavelengths". Journal of Thermal Analysis and Calorimetry 139, 2365–2380,2020.

[33] Kanti PK, Sharma K V., Minea AA, Kesti V. "Experimental and computational determination of heat transfer, entropy generation and pressure drop under turbulent flow in a tube with fly ash-Cu hybrid nanofluid". International Journal of Thermal Science 167, 107016, 2021.

[34] Shengnan C, Jizu L, Peng W, Chengzhi H, Minli B. "Numerical investigation on the influence of particle deposition on nanofluid turbulent flow and heat transfer characteristics". International Communications in Heat and Mass Transfer 126, 105466, 2021.

[35] Shiravi AH, Shafiee M, Firoozzadeh M, Bostani H, Bozorgmehrian M. "Experimental study on convective heat transfer and entropy generation of carbon black nanofluid turbulent flow in a helical coiled heat exchanger. Journal of Thermal Analysis and Calorimetry 145, 597–607, 2021.

[36] Mozafarie SS, Javaherdeh K, Ghanbari O. "Numerical simulation of nanofluid turbulent flow in a double-pipe heat exchanger equipped with circular fins". Journal of Thermal Analysis and Calorimetry 143, 4299–4311, 2021.

[37] Mahani RB, Ahmadi A, Hezaveh HM, Sepehrirad M, Talebizadehsardari P. "Investigating the effects of different innovative turbulators on the turbulent flow field and heat transfer of a multi-phase hybrid nanofluid". Journal of Thermal Analysis and Calorimetry 143, 1755–1772, 2021.

[38] Uysal C. "Which parameter should be used in evaluating nanofluids flows: Reynolds number, velocity, mass flow rate or pumping power?". Heat Transfer Research 51(5), 447-497, 2020.

[39] ANSYS Fluent Theory Guide, 2013.

[40] Incropera FP, Bergman TL, Lavine AS, DeWitt DP. Fundamentals of Heat and Mass Transfer, 7th ed. John Wiley & Sons, Haboken, New Jersey, 2011.

[41] Goudarzi S, Shekaramiz M, Omidvar A, Golab E, Karimipour A, Karimipour A. "Nanoparticles migration due to thermophoresis and Brownian motion and its impact on Ag-MgO/Water hybrid nanofluid natural convection". Powder Technology 375, 493–503, 2020.

[42] Esfe MH, Arani AAA, Rezaie M, Yan WM, Karimipour A. "Experimental determination of thermal conductivity and dynamic viscosity of Ag-MgO/water hybrid nanofluid. International Communications in Heat and Mass Transfer 66, 189–195, 2015.

[43] Gnielinski V. "Neue Gleichungen für den Wärme- und den Stoffübergang in turbulent durchströmten Rohren und Kanälen". Forsch. Ing.-Wes. 41 (1), 8–16, 1975.

[44] Uysal C, Gedik E, Chamkha AJ. "A numerical analysis of laminar forced convection and entropy generation of a diamond-Fe3O4/water hybrid nanofluid in a rectangular minichannel". Journal of Applied Fluid Mechanics 12 (2), 391-402, 2019.